Infrared Hollow Waveguide Sensors for Simultaneous Gas Phase Detection of Benzene, Toluene, and Xylenes in Field Environments

ARTICLE *in* ANALYTICAL CHEMISTRY · MAY 2011

Impact Factor: 5.64 · DOI: 10.1021/ac1031034 · Source: PubMed

analytical chemistry

ARTICLE

pubs.acs.org/ac

Infrared Hollow Waveguide Sensors for Simultaneous Gas Phase Detection of Benzene, Toluene, and Xylenes in Field Environments

Christina R. Young,[†,○] Nicola Menegazzo,[†,▽] Andrew E. Riley,[‡] Cornelius H. Brons,[‡] Frank P. DiSanzo,[§] Jacquelyn L. Givens,[∥] John L. Martin,[⊥] Mark M. Disko,[‡] and Boris Mizaikoff*[,#]

[†]Georgia Institute of Technology, School of Chemistry and Biochemistry, Atlanta, Georgia 30332-0400, United States

[‡]Corporate Strategic Research and [§]Analytical Sciences Laboratory, ExxonMobil Research and Engineering Company, Annandale, New Jersey, 08801

[∥]ExxonMobil Biomedical Sciences Incorporated, Annandale, New Jersey 08801, United States

[⊥]ExxonMobil Medicine and Occupational Health Global, Baytown, Texas 77520, United States

[#]University of Ulm, Institute of Analytical and Bioanalytical Chemistry, 89081 Ulm, Germany

Supporting Information

ABSTRACT:

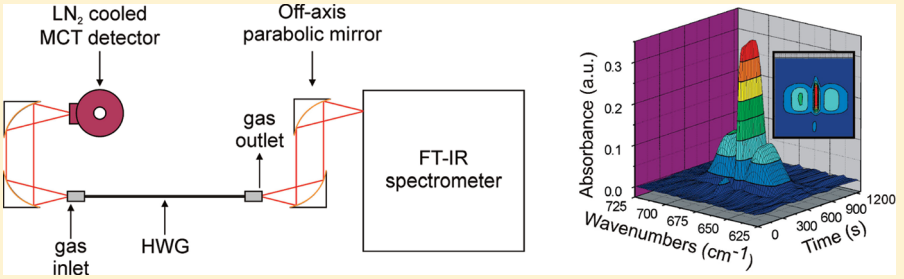

Simultaneous and molecularly selective parts-per-billion detection of benzene, toluene, and xylenes (BTX) using a thermal desorption (TD)-FTIR hollow waveguide (HWG) trace gas sensor is demonstrated here for the first time combining laboratory calibration with real-world sample analysis in field. A calibration range of 100−1000 ppb analyte/N_2 was developed and applied for predicting the concentration of blinded environmental air samples within the same concentration range, and demonstrate close agreement with the validation method used here, GC-FID. The analyte concentration prediction capability of the TD-FTIR-HWG trace gas sensor also compares well with the industrial standard and other experimental techniques including GC-PID, ultrafast GC-FID, and GC-DMS, which were simultaneously operated in the field. With the advent of a quantum cascade laser with emission frequencies specifically tailored to efficiently overlap benzene absorption as the most relevant analyte, the overall sensor footprint could be considerably reduced to ultimately yield hand-held trace gas sensors facilitating direct and real-time detection of BTX in air down to low ppb levels.

INTRODUCTION

To date, there is a high demand for trace gas sensors capable of rapid, sensitive, and selective detection of the gas phase monocyclic aromatic hydrocarbons benzene, toluene, and xylenes (BTX) for applications such as process monitoring,[1] environmental/workplace safety,[2−5] quality assurance/control in commercial processes,[6] and bioremediation efficiency.[7] The primary goal of the work described herein is to develop and characterize rapidly responding sensing strategies with a compact device footprint for selectively and simultaneously detecting these compounds in the low parts per million to parts per billion concentration range. Currently, low parts per billion (ppb) detection for BTX components within an ambient sample is possible, however, this usually requires extended collection and analysis times (>30 min) via e.g., gas chromatographic approaches using mass spectrometry (GC-MS) or flame ionization (GC-FID) as a detector.[8] The ideal sensor-type instrument would determine the BTX components at concentrations <10 ppb in less than a minute, thereby exceeding the current requirements of the American Conference of Governmental Industrial Hygienists (ACGIH) Threshold Limit Value (TLV) of 0.5 ppm for an 8 h workshift and the Occupational Safety and Health (OSHA) regulations (i.e., specifically standard 29 CFR 1910.1000), which sets the permissible exposure limits (8 h time weighted average) of benzene, toluene, and xylenes at 1, 200, and 100 ppm respectively for occupational workers. Furthermore, OSHA sets a short-term exposure limit (15 min) for benzene at 5

Received: November 25, 2010
Accepted: May 25, 2011
Published: May 25, 2011

ppm, and the National Institute for Occupational Safety and Health at 1 ppm (100 ppb). Thus, the ideal trace gas sensor should be capable of not only discretely testing for these constituents, that is BTX detection in grab samples, but should also provide continuous monitoring capabilities over a period of 8 h or more, during which a worker may be exposed to a concentration spike not necessarily apparent by conventional discontinuous measurement techniques or dosimetry. However, it is important to note that dosimetry is successful in the presence of mixtures of hydrocarbons and other volatile chemicals.

The current state-of-the-art for gas phase ppb-level detection of BTX typically utilizes GC for separation/selectivity combined with a variety of detection schemes including photoionization (GC-PID),[8] flame ionization (GC-FID),[9−13] or mass spectrometry (GC-MS),[11,14−18] usually complemented with some form of preconcentration via adsorption, for example PDMS and/or Carboxen. GC-PID is an advantageous technique for the simultaneous detection of BTX mixtures; however, selectivity may suffer from alkane interferences.[19] GC-FID provides volatile organic compound (VOC) analysis with a large linear dynamic range at relatively low cost without unambiguous identification of the detected constituents. To partly overcome this drawback, the separation may be simultaneously performed on two columns with different polarity. GC-MS provides high sensitivity, selectivity, and accuracy with the potential for transportable device footprints,[20] as demonstrated by a study detecting low ppb levels of BTX in urban outdoor environments over space and time gradients.[21] However, GC-MS is limited in providing real-time measurements, is instrumentally expensive, and does not currently exhibit the potential for full miniaturization/integration, which would enable for example detection via wearable badges. Furthermore, all three aforementioned methods have limitations in differentiating between and quantifying *meta*- and *para*-xylenes unless a properly configured GC or GC/MS system is used to resolve *m*- and *p*-xylenes.

In addition to current state-of-the-art methods, other analytical strategies have been developed to measure ppb-levels of BTX. A miniaturized GC system has been combined with a solid-state metal oxide semiconducting (MOX) detector to detect a few ppb up to several tens of ppb BTX in indoor air.[22,23] Another study has differentiated 20 ppb benzene in a BTX gas mixture via a combination of GC with ion mobility spectrometry (IMS).[24] Furthermore, microfluidic devices utilizing mesoporous silicate designed for gas phase BTX sensing[25,26] have been applied for detecting 100 ppb benzene discriminated in a mixture against toluene.[26] Recently, a method known as membrane introduction mass spectrometry (MIMS) was utilized for measuring benzene and toluene at LODs of 600 and 200 ppt respectively without additional separation via GC.[27]

Optical spectroscopy is another analytical platform suitable for ppb detection of gas phase BTX. Kim and co-workers have applied UV differential optical absorption spectroscopy (DOAS)[28] for detecting BTX at low ppb levels within environmental air and have compared the results to simultaneously performed online GC studies.[29,30] Generally, commercial systems utilizing DOAS with a 500 m open path exhibit detection limits of 0.9 ppb for benzene, toluene, and xylene (BTX) with an accuracy of approximately 30%.[31] Although DOAS systems are capable of continuous and sensitive BTX detection, their sensitivity may suffer at low-visibility conditions, and selectivity may be affected by interferences resulting from the presence of oxygen, ozone, and hydrocarbons with similar spectra.[32] Direct spectrophotometry of BTX has been demonstrated at ppb levels using PDMS as a sorbent material.[33]

Fourier-transform infrared (FTIR) spectroscopy is a particularly interesting optical technique due to molecularly specific fundamental rotational and vibrational transitions active in the mid-infrared spectral range, which provide pronounced absorption features conducive for sensitive and selective optical sensing schemes in gas phase analysis in environmental air samples.[34] The IR spectral regime evaluated here focuses on the so-called "fingerprint region" (10−20 μm) where BTX exhibit selective absorption peaks at 673, 727, 740, 795, and 767 cm^{-1}, respectively. Using appropriate calibration, qualitative and quantitative information on specific constituents in the gas phase at ppm to ppb detection levels is achieved.

To enhance the effective optical path length, a hollow waveguide[35] was utilized to propagate mid-infrared radiation from the light source to the detector simultaneously serving as a low-volume, miniaturized gas cell. FTIR spectroscopy taking advantage of hollow waveguides (FTIR-HWG) has previously been demonstrated as a powerful analytical method for gas phase chemical detection with detection limits generally in the low ppm concentration range without preconcentration.[36−41] A preconcentration step based on thermal desorption was used here to further lower the detection limits into the ppb range complying with EPA and OSHA guidelines for measuring BTX in ambient air. Solid phase microextraction (SPME) via graphitized carbon black sorbent tubes has been applied to preconcentrate gas standards or field samples, which were then thermally desorbed as a concentrated gas plume into the HWG. Pogodina, et al. have previously used a similar approach to detect ethene down to approximately 1 ppb in urban air.[41] In the work reported here, we demonstrate ppb detection of BTX with a TD-FTIR-HWG trace gas sensor for the first time both by establishing a robust lab calibration and utilizing this calibration for evaluating blinded real-world field samples in the field. The obtained sensor results were validated by GC-FID and furthermore compared to current off-the-shelf detection devices suitable for field usage, as well as industrial prototypes.

MATERIALS AND METHODS

A robust calibration for ppb BTX was established in a laboratory environment prior to the evaluation of field samples on site. Nine individual certified gas standards (Praxair) for BTX with concentrations of 100, 500, and 1000 ppb/N_2 were individually adsorbed onto graphitized carbon black, and subsequently thermally desorbed into the FTIR-HWG trace gas sensor. On the basis of the calibration procedure, a protocol was designed for obtaining consistent measurement conditions during field measurements. The sorption method consisted of a low-flow sample pump (SKC model 222−3, Eighty Four, PA), which was used to draw certified gas standard samples through a syringe needle that pierced the airtight septum of a Tedlar bag. A syringe needle was used to ensure a completely sealed gas transfer path and, subsequently, to avoid any possible gas leakage arising from sampling directly from the Tedlar bag release valve. All other access ports of the bag including the side arm valve were appropriately sealed. The sample pump withdrew gas from a 10 L capacity Tedlar bag (SKC, Model 232, Eighty Four, PA) across a sorbent tube preconcentrating the sample at a rate of 162 mL/min for 7 min resulting in a volume of 1.1 L of sampled gas. The sample pump flow was calibrated using a manual SKC Model 303 film flow meter (SKC, Eighty Four, PA).

The sorbent tubes used in this study were packed with Carbopack B 40/60 (Supelco Inc., Bellefonte, PA). Graphitized

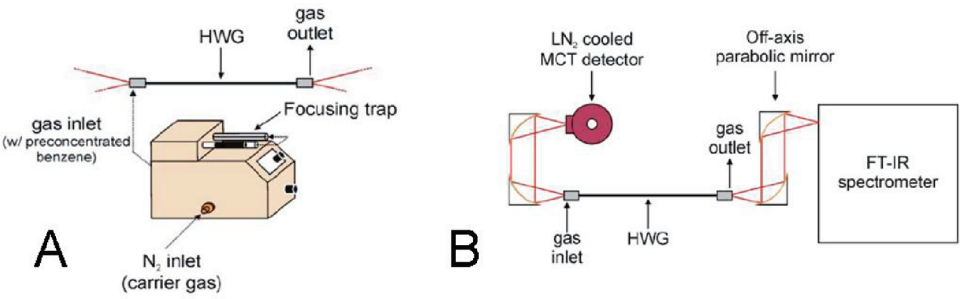

Figure 1. Experimental Setup. (A) Schematic of the overall measurement process. After preconcentration, the sorbent tube (front cylinder with black insert illustrating the sorbent material) was heated to release the analytes onto the focusing trap (rear cylinder). The gas plume was subsequently released into the HWG using a gas inlet and outlet based on custom-made gas cells, which provide a gastight sealing of the HWG. (B) Schematic of the IR sensor setup. IR radiation emanated from the FTIR spectrometer and was focused into the HWG in opposite direction of the gas flow. Following selective analyte absorption, radiation propagating through the HWG was focused onto the MCT detector and an IR spectrum was generated.

carbon black with a 60−80 mesh and a surface area of approximately 100 m^2/g was used. After experimental studies, graphitized carbon black was selected as a suitable sorbent material for BTX based on its ability to selectively adsorb and release BTX while limiting artifacts during the sampling and heating procedure. Tenax TA-packed sorbent tubes (Supelco Inc., Bellefonte, PA) were additionally evaluated, however, contributions to toluene and benzene absorbance features evolved from this polymeric sorbent material, thereby leading to less reliable results at low concentrations.

Thermal desorption was applied here to lower the detection limits to the ppb range with sufficient statistical confidence (10σ). Following BTX adsorption onto the sorbent material, a Dynatherm ACEM 9300 thermal desorption (TD) unit (CDS Analytical, Oxford, PA, USA) was used to desorb enriched analytes of interest from the sorption tube onto a focusing trap at a flow rate of 50 mL/min, and at a temperature of 150 °C for 5 min. The trap was maintained at temperatures <40 °C during collection, and subsequently flash heated to 300 °C for 30 min producing a concentrated gas plume released into the HWG at a slow carrier gas flow rate (<1 mL/min); henceforth referred to as column flow. Part A of Figure 1 schematically illustrates the overall measurement process from the thermal desorption of the preconcentrated sample at the sorbent tube to determining the analyte IR absorbance spectra within the HWG.

Introduction of the concentrated gas plume into the hollow waveguide (2 mm ID, 50 cm length) was achieved by custom-engineered gas cells with a small internal volume (approximately 1 cm^3) and equipped with IR transparent zinc selenide (ZnSe) windows enabling coupling of the IR beam into the waveguide. Incident radiation was externally coupled from a Bruker Matrix M spectrometer (Bruker Optics, Billerica, MA, USA), and directed toward the output gas cell utilizing gold coated off-axis parabolic mirrors (OAPM). Finally, the attenuated radiation emanating from the distal end of the HWG was focused onto a liquid nitrogen cooled mercury−cadmium−telluride (MCT) detector (Infrared Associates Inc., Stuart, FL, USA) yielding a broadband transmission/absorption spectrum (4000 to 600 cm^{-1}). Part B of Figure 1 shows a schematic of this optical setup. The spectrometer was computer controlled and operated from outside of a fume hood. The temperature of the HWG was maintained at approximately 50 °C using a heating jacket (Watlow Electric Manufacturing Co., St. Louis, MO, USA) to minimize potential condensation of BTX or other constituents at the interior HWG surface. All collected spectra correspond to the averaged absorbances from 100 spectra scans recorded at a spectral resolution of 2 cm^{-1}, thus yielding a response time of 39 s.

Field samples were collected directly from ambient air using a Gillian HFS 113A precalibrated high-flow sample pump (Gillian Instrument Corp., NJ, USA) and collected into 25 L Tedlar bags (SKC, Eighty Four, PA, USA) from several undisclosed locations. A volume of approximately 6 L of air sample was then transferred from the initial 25 L bag into individual 10 L Tedlar bags. Unknown air samples were then extracted from one of the 10 L Tedlar bags using the same analysis procedure previously described for establishing the laboratory calibration and subsequently analyzed by the TD-FTIR-HWG trace gas sensor.

Several other instruments were evaluated during this field study simultaneously with the TD-FTIR-HWG trace gas sensor, using the same blinded samples, comprising photoionization detectors (PID; one of which was benzene-specific), a gas chromatograph with a flame ionization detector (GC-FID), a gas chromatograph with a photoionization detector (GC-FID), colorimetric detector tubes, and a gas chromatograph utilizing a photoionization/differential ion mobility spectrometer. The validation method during the field study was GC-FID, with the blinded samples preconcentrated onto a coconut charcoal tube, and desorbed with carbon disulfide.

RESULTS AND DISCUSSION

Part-per-billion level BTX laboratory calibrations were established by integrating the absorbance peaks collected from certified gas standards at known concentrations. Absorbance spectra were obtained from releasing concentrated gas plumes into the HWG. Time-resolved plots of such measurements are shown in parts A−C of Figure 2 for benzene, toluene, and the xylenes respectively, where the inserts illustrate the analyte gas plume entering and exiting the trace gas sensor. Evidently, the absorbance increases to a maximum and subsequently decreases over time. The resolution of this plume is largely dependent on the column flow; that is, an increasing column flow leads to fewer absorption peaks, albeit faster response times, and vice versa. To obtain precise and accurate calibrations, the column flow was optimized until multiple reproducible maximum peaks were observed, which were then integrated for quantitative data evaluation.

Parts A−C of Figure 3 show examples of absorbance spectra for BTX laboratory calibrations. As expected, the absorbances increase linearly with an increase in concentration in agreement with the Beer−Lambert law. The specific spectra shown here represent the maximum signals for the selected concentration. Parts

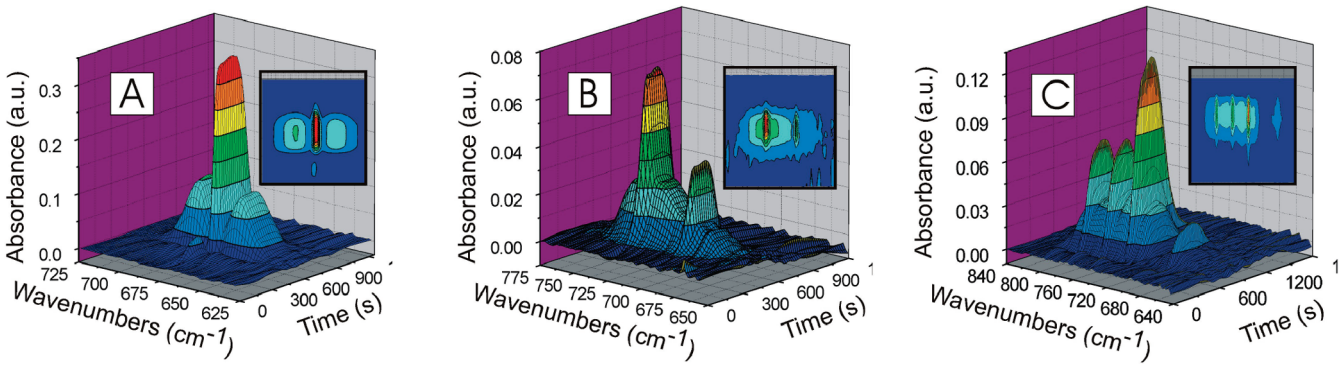

Figure 2. Release of the concentrated BTX gas plume into the HWG as a function of time. Time-resolved 3D plots of the analyte concentration (i.e., absorbance) within the plume migrating through the sensing module (HWG) of the IR trace gas sensor for (A) benzene, (B) toluene, (C) *o,p,m*-xylenes. (Insert) Contour plot of the analyte plume entering and leaving the IR trace gas sensor, blue denotes the lowest absorbance (i.e., concentration) and red denotes the highest absorbance (i.e., concentration) over time.

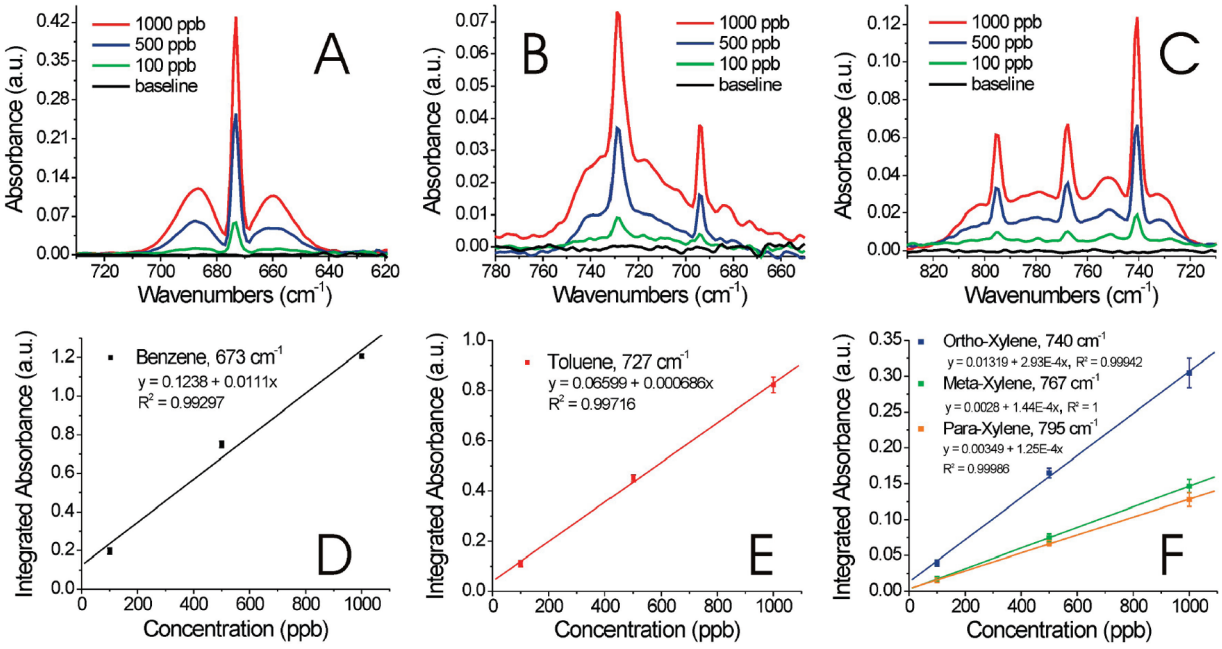

Figure 3. Laboratory calibration of BTX at ppb concentration levels. (A−C) Calibration functions with linear fit correlation coefficients. (D−F) Corresponding absorbance spectra.

D−F of Figure 3 illustrate the correspondingly obtained calibration functions with linear fit correlation coefficients of 0.99297, 0.99716, 0.9942, 1.0000, and 0.9986 for benzene, toluene, and (*o,m,p*)-xylenes respectively exhibiting acceptably low standard deviations with an excellent linear fit. Absorbance values were obtained by integrating the frequency ranges from 677.15−668.01 cm^{-1} for benzene, 762.97−705.30 cm^{-1} for toluene, 744.92−736.41 cm^{-1} for *ortho*-xylene, 771.41−762.24 cm^{-1} for *meta*-xylene, and 799.68−788.53 cm^{-1} for *para*-xylene, respectively. Toluene and xylenes were calibrated after the field studies again under laboratory conditions and then applied to derive the respective concentrations postfield. The thus obtained validated results further demonstrate the superior instrumental robustness of the developed TD-FTIR-HWG trace gas sensor.

Upon completion of laboratory calibration, the instrument was transferred to an undisclosed field measurement location where blinded environmental air samples representative for short-term field readings of these analytes were investigated during a period of one week and compared to the aforementioned analyzers. Prior to daily data collection, a one-point calibration with a known gas standard (Air Liquide America Specialty Gases, Plumsteadville, PA, USA) was performed on site to validate the current instrumental status in comparison to the performance at laboratory conditions. The collected air samples were immediately analyzed by evaluating samples from three individual collection bags per location number. Figure 4a shows an exemplary IR spectrum of a field air sample. It is clearly evident that all five analytes are present in these samples with distinct Q-branch absorbance peaks centered at 673 cm^{-1}, 727 cm^{-1}, 740 cm^{-1}, 767 cm^{-1}, and 795 cm^{-1} corresponding to the molecular signatures of benzene, toluene, and (o,m,p)-xylenes, respectively in the fingerprint region.

GC-FID was used to validate the method reported here via independent analysis of the same field samples after the field

dx.doi.org/10.1021/ac1031034 |*Anal. Chem.* 2011, 83, 6141–6147

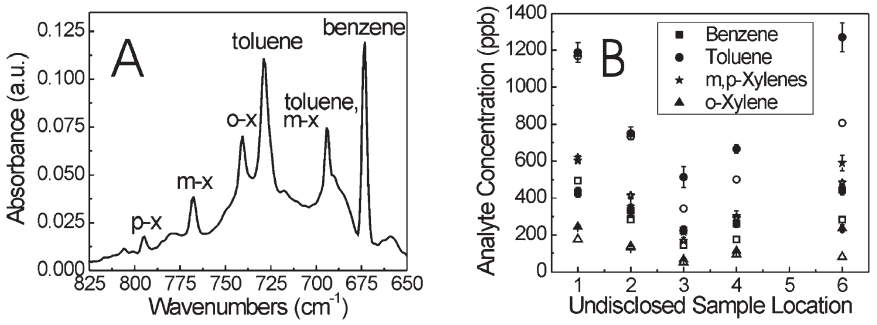

Figure 4. Field measurement results using the TD-FTIR-HWG sensor. (A) Exemplary IR spectrum of a field gas sample. (B) Direct comparison of TD-FTIR-HWG results with GC-FID validation. Solid points represent TD-FTIR-HWG data, and outline points represent GC-FID data.

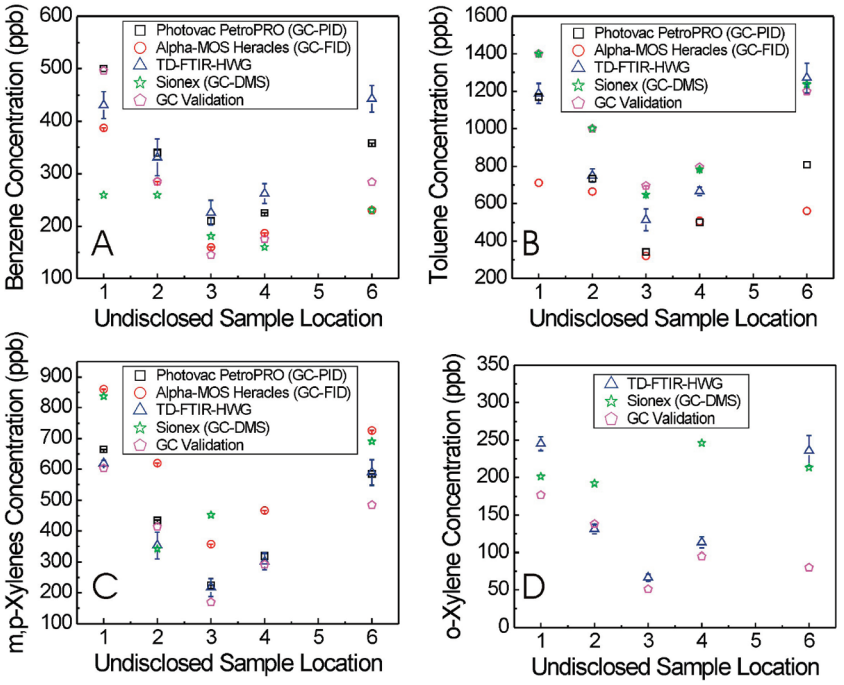

Figure 5. Comparative BTX field study. Predictive capability of the evaluated techniques simultaneously analyzing the same environmental air samples in the field for benzene (A), toluene (B), *meta*- and *para*-xylenes (C), and *ortho*-xylene (D).

measurement campaign at laboratory conditions. Part B of Figure 4 compares the obtained results between the GC-FID validation, and the TD-FTIR-HWG trace gas sensor. It should be emphasized that among the instruments compared in this study, only the TD-FTIR-HWG trace gas sensor was able to successfully quantitatively discriminate all three isomers of xylene, whereas the GC techniques could not distinguish between *meta*-xylene and *para*-xylene. As such, in part B of Figure 4, predicted concentrations for *meta*- and *para*-xylene isomers were summed together also for the TD-FTIR-HWG trace gas sensor, thus enabling direct comparison with the GC technique.

The toluene signal obtained at the TD-FTIR-HWG trace gas sensor appears to provide higher concentration values than the validation method, particularly for location six; this behavior is attributed to the peak overlap and spectral contributions from other analytes in the mixture such as *meta*-xylene and ethylbenzene, with the latter not included in the calibration. However, the future application of multivariate calibration models in lieu of univariate calibration following these first successful field studies is expected to significantly improve the accuracy of the predicted toluene concentrations.

It should be noted that data from location 5 was excluded from the considerations herein, as this sample revealed significantly more variation between the different analysis techniques. After thorough evaluation, it was found that in contrast to all other locations sample five was prepared and analyzed the day after the sample bag was collected by GC-FID validation most likely leading to irreproducible effects. A Grubb's test at the 5% significance level on the range between sample averages for the various techniques for the other six samples indicates that, on this basis, sample 5 may reasonably be rejected ($G\ 1.697 > 1.580$, $\alpha = 5\%$) as an outlier within this data set; therefore, this sample was not considered as representative within the collected data set. Data for toluene and *meta*-/*para*-xylenes have confirmed the Grubb's test results obtained for benzene in sample 5.

Figure 5 describes the predictive capability of the TD-FTIR-HWG trace gas sensors in comparison with the other instrumental techniques that were operated during this field test and

dx.doi.org/10.1021/ac1031034 |*Anal. Chem.* 2011, 83, 6141–6147

which have simultaneously analyzed the same field samples. With the exception of location 6, the TD-FTIR-HWG sensor predicts analyte concentrations within ±100 ppb of the validation method, which is comparable to or better than the other tested devices including commercial analyzers. It should be noted that the sampling parameters presented in here were specifically tailored to be compatible with the field trial requirements. For maximizing the sensitivity of TD-FTIR-HWG sensors, experimental parameters such as the preconcentration time (gas volume enrichment), the spectral resolution, and the column flow (plume resolution) may be optimized to further lower the detection limits of this sensing device to subppb concentration levels. A preliminary optimization performed in the course of this study already shows the ability of TD-FTIR-HWG sensors to detect 5 ppb of benzene with an integrated absorbance reproducibly above the limit of quantification (according to the 6σ-criterion, i.e., the analytical signal is at least 6 times larger than the standard deviation of the background noise). Measurements of 5 ppb were achieved by increasing the spectral resolution to 1 cm^{-1}, by reducing column flow (<1 mL/min), and averaging 50 spectra resulting in a response time of 43 s per spectrum. Spectral results detailing the detection of 5 ppb benzene compared to the response for 100 and 500 ppb benzene are shown in Figure S1 of the Supporting Information.

CONCLUSIONS

The TD-FTIR-HWG sensor system used here demonstrates the capability of mid-infrared spectroscopy as a portable and powerful tool to directly quantify and discriminate structurally related constituents (BTX) at ppb levels within real-world environmental air samples in the field based on robust laboratory calibrations. This technique compares well to both the GC-FID validation method as well as off-the-shelf analyzers and sensor prototypes based on a variety of measurement principles. It is anticipated that the detection of BTX will improve in both accuracy and precision with the advent of quantum cascade lasers emitting at the relevant wavelengths within the fingerprint regime of the mid-infrared spectrum (>10 μm). Thus, limits of detection within the ppb range without preconcentration may be achieved due to the enhanced spectral density of the IR source efficiently overlapping the absorbance feature of interest, while maintaining the inherent selectivity of the MIR spectral regime, as previously demonstrated with QCL-HWG trace gas sensors designed for other analytes.[42−44]

ASSOCIATED CONTENT

Supporting Information. FTIR spectra of 500, 100, and 5 ppb benzene are shown. Measurements of 500 and 100 ppb benzene were collected at the previously described measurement conditions of 2 cm^{-1} spectral resolution averaging 100 scans resulting in a response time of 42 s. Measurements of 5 ppb benzene were achieved by optimizing the spectral resolution to 1 cm^{-1} averaging 50 scans again resulting in a response time of 43 s. To obtain a statistically significant signal-to-noise ratio, the preconcentration time was increased to 40 min using the same pump flow rate (162 mL/min) as previously used during field measurements. This material is available free of charge via the Internet at http://pubs.acs.org.

AUTHOR INFORMATION

Corresponding Author

*Tel.: +49-731-50-22750; E-mail: boris.mizaikoff@uni-ulm.de.

Present Addresses

○U.S. Food and Drug Administration, Center for Tobacco Products, Office of Science, Rockville, MD 20850.

▽University of Delaware, Department of Chemistry and Biochemistry, Newark, DE 19716.

ACKNOWLEDGMENT

ExxonMobil Research and Engineering Company (EMRE) and ExxonMobil Biomedical Sciences, Inc. are acknowledged for their support of this study. The authors thank Paul Russo, Eileen Pearlman, Justin Davenport, Eduardo Shaw, Rob Tutt, Jeffery Butler, Michael Veraa, Larry Daniel, Tammy Leach, and Steve McGovern (ExxonMobil Chemicals and Medical and Occupational Health departments) who were instrumental in preparing for and executing the field measurement campaign.

REFERENCES

(1) Heger, H. J.; Zimmermann, R.; Dorfner, R.; Beckmann, M.; Griebel, H.; Kettrup, A.; Boesl, U. *Anal. Chem.* **1999**, *71*, 46–57.
(2) Lin, C.-W. *Water, Air, Soil Pollut.* **2001**, *128*, 321–337.
(3) Iovino, P.; Polverino, R.; Salvestrini, S.; Capasso, S. *Environmental Monitoring and Assessment* **2009**, *150*, 437–444.
(4) Gariazzo, C.; Pelliccioni, A.; Di Filippo, P.; Sallusti, F.; Cecinato, A. *Water, Air, Soil Pollut.* **2005**, *167*, 17–38.
(5) Lee, C.; Kim, Y. J.; Hong, S.-B.; Lee, H.; Jung, J.; Choi, Y.-J.; Park, J.; Kim, K.-H.; Lee, J.-H.; Chun, K.-J.; Kim, H.-H. *Water, Air, Soil Pollut.* **2005**, *166*, 181–195.
(6) Volz-Thomas, A.; Slemr, J.; Konrad, S.; Schmitz, T. H.; Apel, E. C.; Mohnen, V. A. *J. Atmos. Chem.* **2002**, *42*, 255–279.
(7) Yeom, S.-H.; Daugulis, A. J. *Biotechnol. Lett.* **2001**, *23*, 467–473.
(8) Kim, K.-H.; Pandey, S. K.; Pal, R. *J. Sep. Sci.* **2009**, *32*, 549–558.
(9) Elke, K.; Jermann, E.; Begerow, J.; Dunemann, L. *J. Chromatogr., A* **1998**, *826*, 191–200.
(10) Kalabokas, P. D.; Hatzianestis, J.; Bartzis, J. G.; Papagiannakopoulos, P. *Atmos. Environ.* **2001**, *35*, 2545–2555.
(11) Augusto, F.; Koziel, J.; Pawliszyn, J. *Anal. Chem.* **2001**, *73*, 481–486.
(12) Koziel, J.; Jia, M.; Pawliszyn, J. *Anal. Chem.* **2000**, *72*, 5178–5186.
(13) Parreira, F. V. *J. Chromatogr. Sci.* **2002**, *40*, 122.
(14) Tumbiolo, S.; Gal, J. F.; Maria, P. C.; Zerbinati, O. *Anal. Bioanal. Chem.* **2004**, *380*, 824–830.
(15) Larroque, V.; Desauziers, V.; Mocho, P. *J. Environ. Monit.* **2006**, *8*, 106–111.
(16) Tumbiolo, S.; Gal, J. F.; Maria, P. C.; Zerbinati, O. *Ann. Chim.* **2005**, 95.
(17) Gorlo, D.; Zygmunt, B.; Dudek, M.; Jaszek, A.; Pilarczyk, M.; Namie nik, J. *Anal. Bioanal. Chem.* **1999**, *363*, 696–699.
(18) Larroque, V.; Desauziers, V.; Mocho, P. *Anal. Bioanal. Chem.* **2006**, *386*, 1457–1464.
(19) Atienza, J.; Aragón, P.; Herrero, M. A.; Puchades, R.; Maquieira, Á. *Crit. Rev. Anal. Chem.* **2005**, *35*, 317–337.
(20) Santos, F. J.; Galceran, M. T. *J. Chromatogr., A* **2003**, *1000*, 125–151.
(21) Meuzelaar, H. L. C.; Dworzanski, J. P.; Arnold, N. S.; McClennen, W. H.; Wager, D. J. *Field Anal. Chem. Technol.* **2000**, *4*, 3–13.
(22) Zampolli, S.; Elmi, I.; Stürmann, J.; Nicoletti, S.; Dori, L.; Cardinali, G. C. *Sens. Actuators, B* **2005**, *105*, 400–406.
(23) Zampolli, S.; Elmi, I.; Mancarella, F.; Betti, P.; Dalcanale, E.; Cardinali, G. C.; Severi, M. *Sens. Actuators, B* **2009**, *141*, 322–328.
(24) Leonhardt, J. W. *J. Radioanal. Nucl. Chem.* **2003**, *257*, 133–139.
(25) Ueno, Y.; Horiuchi, T.; Niwa, O.; Zhou, H. S.; Yamada, T.; Honma, I. *Sens. Actuators, B* **2003**, *95*, 282–286.
(26) Ueno, Y.; Tate, A.; Niwa, O.; Zhou, H. S.; Yamada, T.; Honma, I. *Anal. Bioanal. Chem.* **2005**, *382*, 804–809.

(27) Sokol, E.; Edwards, K. E.; Qian, K.; Cooks, R. G. *Analyst* **2008**, *133*, 1064–1071.
(28) Platt, U.; Perner, D.; Pätz, H. W. *J. Geophys. Res., [Atmos.]* **1979**, *84*, 6329–6335.
(29) Kim, K. H. *Environ. Eng. Sci.* **2004**, *21*, 181–194.
(30) Lee, C.; Kim, Y. J.; Hong, S. B.; Lee, H.; Jung, J.; Choi, Y. J.; Park, J.; Kim, K. H.; Lee, J. H.; Chun, K. J. *Water, Air, Soil Pollut.* **2005**, *166*, 181–195.
(31) Schäfer, K. *Air & Space Europe* **2001**, *3*, 104–108.
(32) Badjagbo, K.; Sauvé, S.; Moore, S. *Trends Anal. Chem.* **2007**, *26*, 931–940.
(33) Lamotte, M.; de Violet, P.; Garrigues, P.; Hardy, M. *Anal. Bioanal. Chem.* **2002**, *372*, 169–173.
(34) Mizaikoff, B. *Anal. Chem.* **2003**, *75*, 258A–267A.
(35) Harrington, J. A. *Fiber and Integrated Optic* **2000**, *19*, 211–227.
(36) Charlton, C.; Thompson, B. T.; Mizaikoff, B. In *Springer Series on Chemical Sensors and Biosensors*; Orellana, G., Moreno-Bondi, M. C., Eds.; Springer-Verlag: Heidelberg, 2005; Vol. 3, pp 133−167.
(37) de Melas, F.; Pustogov, V. V.; Croitoru, N.; Mizaikoff, B. *Appl. Spectrosc.* **2003**, *57*, 600–606.
(38) Thompson, B. T.; Inberg, A.; Croitoru, N.; Mizaikoff, B. *Appl. Spectrosc.* **2006**, *60*, 266–271.
(39) Thompson, B. T.; Mizaikoff, B. *Appl. Spectrosc.* **2006**, *60*, 272–278.
(40) Young, C.; Kim, S.-S.; Mizaikoff, B. In *Lasers in Chemistry*; Lackner, M., Ed.; Wiley-VCH: Weinhem, 2008.
(41) Pogodina, O. A.; Pustogov, V. V.; de Melas, F.; Haberhauer-Troyer, C.; Rosenberg, E.; Puxbaum, H.; Inberg, A.; Croitoru, N.; Mizaikoff, B. *Anal. Chem.* **2004**, *76*, 464–468.
(42) Charlton, C.; de Melas, F.; Inberg, A.; Croitoru, N.; Mizaikoff, B. *IEE Proceedings: Optoelectronics* **2003**, *150*, 306–309.
(43) Charlton, C.; Temelkuran, B.; Dellemann, G.; Mizaikoff, B. *Appl. Phys. Lett.* **2005**, *86*, 194102/194101–194102/194103.
(44) Young, C.; Kim, S.-S.; Luzinova, Y.; Weida, M.; Arnone, D.; Takeuchi, E.; Day, T.; Mizaikoff, B. *Sens. Actuators, B* **2009**, *140*, 24–28.

■ NOTE ADDED AFTER ASAP PUBLICATION

This paper was published on the Web on June 29, 2011 with minor text errors. The corrected version including the addition of a present address for the first author was reposted on July 15, 2011.